Cellular Signalling 108 (2023) 110717

Contents lists available at ScienceDirect

Cellular Signalling

journal homepage: www.elsevier.com/locate/cellsig

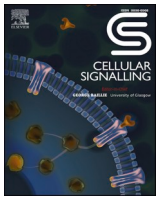

STAT1/3 signaling suppresses axon degeneration and neuronal cell death through regulation of NAD$^+$-biosynthetic and consuming enzymes

Hitoshi Murata *, Yu Yasui, Kazuma Oiso, Toshiki Ochi, Nahoko Tomonobu, Ken-ichi Yamamoto, Rie Kinoshita, Masakiyo Sakaguchi

Department of Cell Biology, Okayama University Graduate School of Medicine, Dentistry and Pharmaceutical Sciences, 2-5-1 Shikata-cho, Kita-ku, Okayama 700-8558, Japan

ARTICLE INFO

Keywords:
NMNAT2
SARM1
NAD$^+$
STAT1/3
IFN-γ

ABSTRACT

Nicotinamide adenine dinucleotide (NAD)$^+$-biosynthetic and consuming enzymes are involved in various intracellular events through the regulation of NAD$^+$ metabolism. Recently, it has become clear that alterations in the expression of NAD$^+$-biosynthetic and consuming enzymes contribute to the axonal stability of neurons. We explored soluble bioactive factor(s) that alter the expression of NAD$^+$-metabolizing enzymes and found that cytokine interferon (IFN)-γ increased the expression of nicotinamide nucleotide adenylyltransferase 2 (NMNAT2), an NAD$^+$-biosynthetic enzyme. IFN-γ activated signal transducers and activators of transcription 1 and 3 (STAT1/3) followed by c-Jun N-terminal kinase (JNK) suppression. As a result, STAT1/3 increased the expression of NMNAT2 at both mRNA and protein levels in a dose- and time-dependent manner and, at the same time, suppressed activation of sterile alpha and Toll/interleukin receptor motif-containing 1 (SARM1), an NAD$^+$-consuming enzyme, and increased intracellular NAD$^+$ levels. We examined the protective effect of STAT1/3 signaling against vincristine-mediated cell injury as a model of chemotherapy-induced peripheral neuropathy (CIPN), in which axonal degeneration is involved in disease progression. We found that IFN-γ-mediated STAT1/3 activation inhibited vincristine-induced downregulation of NMNAT2 and upregulation of SARM1 phosphorylation, resulting in modest suppression of subsequent neurite degradation and cell death. These results indicate that STAT1/3 signaling induces NMNAT2 expression while simultaneously suppressing SARM1 phosphorylation, and that both these actions contribute to suppression of axonal degeneration and cell death.

1. Introduction

Nicotinamide adenine dinucleotide (NAD$^+$), a classical coenzyme, is present in all living cells and plays a central role in redox reactions. Recently, it has become clear that a severe reduction of NAD$^+$ levels that is rigidly regulated by the balance of expressions and activities of enzymes that function in the cellular synthesis and consumption of NAD$^+$ plays a major role in axon degeneration [1–3]. Axon degeneration is an etiological event in neurological disorders, and whose progression disrupts neural networks, resulting in several neurodegenerative disease conditions, including Alzheimer's disease, Amyotrophic lateral sclerosis, Parkinson's disease, and neuropathies [1,4,5], and therefore a deep understanding of the molecular mechanisms of axonal degeneration is an important step for elucidating the causes of neurological disorders and developing innovative therapeutic methods that can be used in common against multiple such disorders. Mammals use nicotinamide as a main ingredient of NAD$^+$ and utilize the salvage pathway that synthesizes NAD$^+$ through a two-step enzymatic reaction. In the first step, nicotinamide phosphoribosyltransferase (NAMPT) converts nicotinamide (NAM) to nicotinamide mononucleotide (NMN). The produced NMN is then metabolized by NMNATs with the help of ATP, which finally gives NAD$^+$. Three NMNAT isoforms have been identified in mammals, all three isoforms are expressed in the neuronal cells in the nervous system. The three isoforms cooperatively function in neuroprotection through their distinct subcellular localizations by maintaining sufficient amounts of NAD$^+$ in each cellular compartment

Abbreviations: CIPN, Chemotherapy-induced peripheral neuropathy; IFN-γ, Interferon gamma; IL-6, Interleukin-6; JNK, c-Jun N-terminal kinase; NAD$^+$, Nicotinamide adenine dinucleotide; NAMPT, Nicotinamide phosphoribosyltransferase; NMNAT2, Nicotinamide nucleotide adenylyltransferase 2; SARM1, Sterile alpha and Toll/interleukin receptor motif-containing 1; STAT, Signal transducers and activators of transcription.

* Corresponding author.
E-mail address: murata@md.okayama-u.ac.jp (H. Murata).

https://doi.org/10.1016/j.cellsig.2023.110717
Received 20 January 2023; Received in revised form 11 May 2023; Accepted 12 May 2023
Available online 13 May 2023

[6]. NMNAT1 is localized to the nucleus, NMNAT2 is present in the Golgi, cytoplasm, and axon, and NMNAT3 is present in mitochondria [6–9]. Among the three isoforms, NMNAT2 plays the greatest role in the axonal degeneration of neurons [2]. NMNAT2 is a labile protein that is rapidly degraded by various stress stimuli [10,11]. Therefore, an effective method to prevent NMNAT2 collapse at the protein level is considered a potential strategy to protect the neuronal cells from the threat of axonal degeneration by preserving an ample amount of NAD^+. Post-translational modifications of NMNAT2, such as palmitoylation or ubiquitination, have been reported to alter the stability of the protein [8,12–15]. On the other hand, transcriptional regulation of NMNAT2 is also an important consideration when contemplating a method for supplying NMNAT2 to cells. However, in contrast to the relatively large number of studies on NMNAT2 at the protein level, the regulatory mechanism(s) of NMNAT2 at the transcriptional level have not been studied in detail.

In addition to the aforementioned NAD^+-synthesizing enzymes, regulation(s) of NAD^+-consuming enzymes plays a pivotal role in maintaining intracellular NAD^+ balance. Poly (ADP-ribose) polymerase (PARP), Sirtuin, and CD38 are known as NAD^+-consuming enzymes, and they take part in several cellular processes, such as DNA repair, transcription control by deacetylation, and Ca^{2+} signal regulation [16–18]. In addition to these proteins, much attention has recently turned to SARM1 as a novel molecule that consumes NAD^+ in neurons and induces axonal degeneration [19,20]. Although SARM1 remains in an inactive state in cells under physiologically normal conditions, the active form functions to fiercely degrade NAD^+ when the intracellular NAD^+ concentration balance is disturbed under several stress conditions, resulting in a severe reduction of NAD^+ [21–23]. As one of the mechanisms leading to the active form of SARM1, we previously reported that the phosphorylation modification of SARM1 at Ser548 by JNK, which regulates the NAD^+-cleavage activity of SARM1 and inhibits mitochondrial respiration at the same time [24]. Thus, inhibition of SARM1 activation is also one of the main options for suppressing the harmful decrease in NAD^+ levels and protecting axons in several neural etiological and pathological processes.

Axon degeneration is also one of the toxic side effects of cancer therapies. Chemotherapy-induced peripheral neuropathy (CIPN) frequently occurs as a side effect of chemotherapy. If the symptoms progress, the anticancer drug dose must be reduced or the drug treatment must be ended, which has a significant negative impact on the patient's quality of life and survival. To date there are no preventive treatments for CIPN [25]. Duloxetine, an antidepressant medicine known as a serotonin-noradrenaline reuptake inhibitor, is administered to improve symptoms, but its efficacy is limited and thus there is urgent need for development of an effective new medicine. Some anticancer drugs targeting microtubules exert strong antitumor effects by inhibiting cancer cell division, but such drugs can also act on the microtubules in neuronal cells as well as cancer cells, resulting in high levels of axonal degeneration and neuronal cell death, and causing CIPN. Therefore, elucidation of the molecular-level mechanism by which anticancer drugs induce cell death via axonal degeneration would be useful for the development of effective CIPN medicines that could be used as a cocktail with anticancer drugs. Previous studies have shown that a decrease in expression of *NMNAT2* gene reduced cell viability in response to anticancer drugs [26]. It has also been reported that NAD^+-consuming SARM1-knockout mice show resistance to various anticancer drug-induced CIPNs [27–29]. These facts suggest that NMNAT2, SARM1, and their relevant molecular pathways are tightly involved in CIPN-induced axonal degeneration. Considering that the suppression of either CIPN-induced NMNAT2 downregulation or SARM1 activation preserves intracellular NAD^+ levels, it seems reasonable to expect that strategies for targeting either of these molecules would be equally effective in preventing CIPN.

Soluble bioactive factors such as growth factors and cytokines regulate intracellular signaling pathways of cell death and survival, which in turn control dozens of transcriptional regulations of genes relevant to the fates of neuronal cells and other cell types. In this study, we explored candidate soluble factor(s) that positively regulate NAD^+ synthesis by regulating of NMNAT2 and SARM1. We identified a single cytokine, IFN-γ, that increases the expression of NMNAT2. IFN-γ activated signal transducers and activators of transcription 1 and 3 (STAT1/3) pathway followed by c-Jun N-terminal kinase (JNK) suppression. We found that STAT1/3 activation increased the expression of NMNAT2 at both mRNA and protein levels and, at the same time, suppressed the activation of SARM1. Vincristine, an anticancer drug that inhibits microtubule formation and is known to cause CIPN, was found to induce the degradation of NMNAT2 and phosphorylation of SARM1. In contrast, IFN-γ-mediated STAT1/3 activation inhibited these events and modestly suppressed neurite degradation and apoptosis. Thus, this study is the first to describe new neuronal role of STAT1/3. Namely, STAT1/3 signaling regulates NAD^+ metabolism by promoting two inverse events upregulation of NAD^+ synthesis and downregulation of NAD^+ consumption through regulation of the expression of NMNAT2 and SARM1. In this way, STAT1/3 plays a critical role in protecting neurons from the threat of axonal degeneration under stress conditions, including CIPN.

2. Materials and methods

2.1. Chemicals and antibodies

IFN-γ, EGF, GDF-3 and IL-22 were purchased from R&D systems. IFN-α was purchased from Cell Signaling Technologies (CST). IFN-β and FGF2 were purchased from Pepro Tech. BDNF and GDNF were purchased from Cell Guidance Systems. IL-6 was purchased from Proteintech. Niclosamide and Stattic were purchased from Med Chem Express. Vincristine sulfate was purchased from Fujifilm Wako Chemicals. The following antibodies were used: mouse anti-NMNAT2 (Santa Cruz Biotechnology, Santa Cruz, CA, cat# sc-515,206, dilution 1:100 in Can Get Signal Solution 1 [Toyobo, Osaka, Japan]), rabbit anti-SARM1 (CST, cat# 13022, dilution 1:500 in Can Get Signal Solution 1), rabbit anti-STAT1 (CST, cat# 14994, dilution 1:1000 in Can Get Signal Solution 1), rabbit anti-phospho-STAT1 (CST, cat# 7649, dilution 1:1000 in Can Get Signal Solution 1), mouse anti-STAT3 (CST, cat# 9139, dilution 1:500 in Can Get Signal Solution 1), rabbit anti-phospho-STAT3 (CST, cat# 9145, dilution 1:500 in Can Get Signal Solution 1), rabbit anti-JNK (CST, cat#9252, dilution 1:500 in Can Get Signal Solution 1), mouse anti-phospho-JNK (CST, cat#9255, dilution 1:500 in Can Get Signal Solution 1), rabbit anti-c-Jun (CST, cat# 9165, dilution 1:500 in Can Get Signal Solution 1), rabbit anti-phospho-c-Jun (CST, cat# 3270, dilution 1:500 in Can Get Signal Solution 1), rabbit anti-NMNAT1 (CST, cat# 98354, dilution 1:500 in Can Get Signal Solution 1), mouse anti-Neurofilament-M ([NF-M] CST, cat# 2838, dilution 1:1000 in 10% skim milk), rabbit anti-cleaved caspase-3 ([Cl. Caspase3] CST, cat# 9664, dilution 1: 330 in Can Get Signal Solution 1), mouse anti-Neurofilament-L ([NF-L] Santa Cruz Biotechnology, cat# sc-20,012, dilution 1:1000 in 10% skim milk), mouse anti-NAMPT (Santa Cruz Biotechnology, cat# sc-393,444, dilution 1:1000 in Can Get Signal Solution 1), and mouse anti-β-Actin (Sigma-Aldrich, Cat #A2228, dilution 1:20000 in 10% skim milk).

A mouse monoclonal antibody (mAb) against phospho-Ser548 SARM1 (dilution 1:500 in 3% bovine serum albumin/Tris-buffered saline, 0.1% Tween 20) was generated by ITM Co. (Matsumoto, Japan). The mAb was produced by immunizing animals with a synthetic phospho-peptide corresponding to residues surrounding Ser548 of human SARM1 (AAREMLHpSPLPCTGG).

2.2. Cell culture

SH-SY5Y cells were cultured in DMEM/F12 medium (Thermo Fisher Scientific) supplemented with 10% fetal bovine serum (FBS). To obtain human matured neuronal cells in a culture system, 201B7 induced

pluripotent stem cells (iPSCs) derived from a healthy donor (a 36-year-old female; RIKEN BRC [Tsukuba, Japan]) were used and were differentiated according to the established protocol as described previously. Induction of neural stem cells (NSCs) from iPSCs was done using PSC neural induction medium (Thermo Fisher Scientific) according to the manufacturer's instructions. After neural induction for 7 days, P0 NSCs were expanded in neural expansion medium on a coated dish with Geltrex LDEV-Free hESC-qualified reduced growth factor basement membrane matrix (Thermo Fisher Scientific). To make the Geltrex-coated dish, a dish was incubated with Geltrex matrix solution (1:100 with Neurobasal medium) for 1 h. For differentiation into neurons, NSCs were cultured at a density of 1×10^5 cells/cm^2 on a 0.002% poly-L-lysine (Sigma-Aldrich) and 10 μg/ml laminin (Thermo Fisher Scientific)-coated dish in Neurobasal plus medium (Thermo Fisher Scientific) supplemented with 2% B-27 plus supplement (Thermo Fisher Scientific), 2 mM GlutaMAX supplement (Thermo Fisher Scientific), CultureOne supplement (Thermo Fisher Scientific) and 200 μM ascorbic acid (Sigma-Aldrich). Spent medium was changed every 3 days and the cells were used each experiment from day 6.

The pSAKA-1B vector (1B) was used to obtain stable transformants of NSCs [30]. To establish the gene-engineered NSCs that overexpress NMNAT2, NSCs were transfected with a set of plasmids, including the 1B-NMNAT2, the 1B-transposase, and the 1B-puromycin resistance gene plasmids, using Lipofectamine Stem Transfection Reagent (Thermo Fisher Scientific). The 1B-empty-gene plasmid was used to obtain control NSCs instead of the 1B-NMNAT2 plasmid. To establish the other gene-engineered NSCs that own a gene signature with a low level of NMNAT2 and a high level of SARM1 in expressions, NSCs were transfected with the TrueGuide synthetic guide RNA targeting NMNAT2 (Thermo Fisher Scientific, cat#A35533) and the Cas 9 Protein V2 (Thermo Fisher Scientific), with an additional set of plasmids containing the 1B-SARM1, the 1B-transposase, and the 1B-puromycin resistance gene plasmids, using Lipofectamine Stem Transfection Reagent. To obtain control NSCs, the 1B-empty-gene plasmid was used for the 1B-SARM1 plasmid without transfection of guide RNA. After 48 h, the transfected NSCs were treated with 0.5 mg/ml puromycin, and the survived puromycin-resistant NSCs were collected. Then, they were differentiated into neurons by the same procedures described above.

2.3. Microfluidic cultures

Microfluidic chambers, specifically Standard Neuron Devise (SND450, [Xona Microfluidics]), were placed onto 0.5 mg/ml poly-L-lysine (Fujifilm Wako Chemicals)- and 10 μg/ml laminin-coated glasses. Cell suspension (1×10^5 cells) was pipetted into the top well of the device, and the spent medium was changed every four days. On day 12, IFN-γ was added to both compartments (cell bodies side and axonal side) to be the final concentration of it at 0 or 100 ng/ml for 24 h. Vincristine was added only to the axonal compartment to 0 or 50 nM in culture and incubated for another 24 h in the presence of IFN-γ. Bright-field images of cells growing in microfluidic chambers were obtained using a Keyence BZ-X700 microscope. To quantify the axon degeneration rate, the individual axons formed in this experimental context were all scanned, and their conditions in the images were then analyzed using ImageJ software.

2.4. Real-time qPCR

Total RNA was prepared using an SV Total RNA Isolation System (Promega Biosciences). First-strand cDNA synthesis was performed with total RNA using a SuperScript III First-Strand Synthesis System for RT-PCR (Thermo Fisher Scientific). Synthesized cDNA was used for the PCR analysis with a TaqMan Gene Expression Assay (Thermo Fisher Scientific) targeting NMNAT2 (Hs00322752_m1), SARM1 (Hs00248344_m1) and glyceraldehyde 3-phosphate dehydrogenase ([GAPDH] Hs02758991_g1). Relative expression levels were calculated using the ΔCt method, normalized against GAPDH as an internal control and analyzed using StepOnePlus software (Thermo Fisher Scientific).

2.5. Western blot analysis

Western blot analysis was performed under conventional conditions after lysing cells using an SDS sample buffer with PhosphoSTOP (Roche). Each five μg of protein extract was separated by SDS-polyacrylamide gel electrophoresis and electro-transferred onto an Immobilon membrane (Millipore). To detect immunoreactive proteins, we used HRP-conjugated anti-mouse or anti-rabbit secondary antibodies (CST) and Pierce Western Blotting Substrate Plus (Thermo Fisher Scientific). To quantify the protein level of NMNAT2, NF-M, and NF-L, the individual band images of proteins were scanned and analyzed using ImageJ software. Then, their intensities were normalized against β-Actin as an internal control.

2.6. NAD^+ assay

A Cell Count Normalization Kit (Dojindo) was used to normalize cell numbers before the NAD^+ assay. The fluorescence intensity of cells stained with Hoechst 33342 was detected by FlexStation 3 (Molecular Devices; Ex: 350 nm; Em: 461 nm). An NAD/NADH-Glo assay (Promega Biosciences) was used to analyze NAD^+ levels. Cells were incubated with NAD/NADH-Glo reagent for 30 min according to the manufacturer's instructions. The luminescence intensity of cells incubated with NAD/NADH-Glo reagent was detected by Fluoroskan Ascent FL (Thermo Fisher Scientific). NAD^+ levels were normalized by the fluorescence of Hoechst 33342.

2.7. Cell viability assay

A CellTiter-Glo assay (Promega Biosciences) was used to analyze cell viability. Cells were incubated with CellTiter-Glo detection reagent for 10 min according to the manufacturer's instructions. Luminescence was observed using a Fluoroskan Ascent FL (Thermo Fisher Scientific). Cell viability was calculated with the control group at 100%.

2.8. Statistical analysis

Prior to statistical analysis, each experiment was repeated three times. The results are expressed as means +/− S.D. All statistical analyses were performed with EZR (Saitama Medical Center, Jichi Medical University, Saitama, Japan), which is a graphical user interface for R (The R Foundation for Statistical Computing, Vienna, Austria) [31]. One way and two-way ANOVA were used for comparison. If the ANOVA showed a significant difference, Tukey's test was used as a post hoc test. p values of <0.05 were considered statistically significant.

3. Results

3.1. Screening for soluble factor(s) that induce NMNAT2 expression

In order to search for a soluble bioactive factor(s) that has the potential to upregulate the expression of NMNAT2, a NAD^+ synthesizing enzyme, in neuronal cells, a total of seven factors that are expected to act on neuronal survival, were individually added to a culture of human induced pluripotent stem cell (iPSC)-derived neurons, and the treated cells were then analyzed by qPCR and WB for their expressions of NMNAT2. This screening showed that IFN-γ was the only one of the seven factors that increased NMNAT2 at both the mRNA and protein levels (Fig. 1(a and c)). IFN-γ induced an approximately 1.5-fold increase in-*NMNAT2* mRNA expression, and an approximately 8-fold increase in the protein expression (Fig. 1(a and d)). On the other hand, the expression level of SARM1, a NAD^+-consuming enzyme, showed no any appreciable change by treatment with the same series of soluble factors

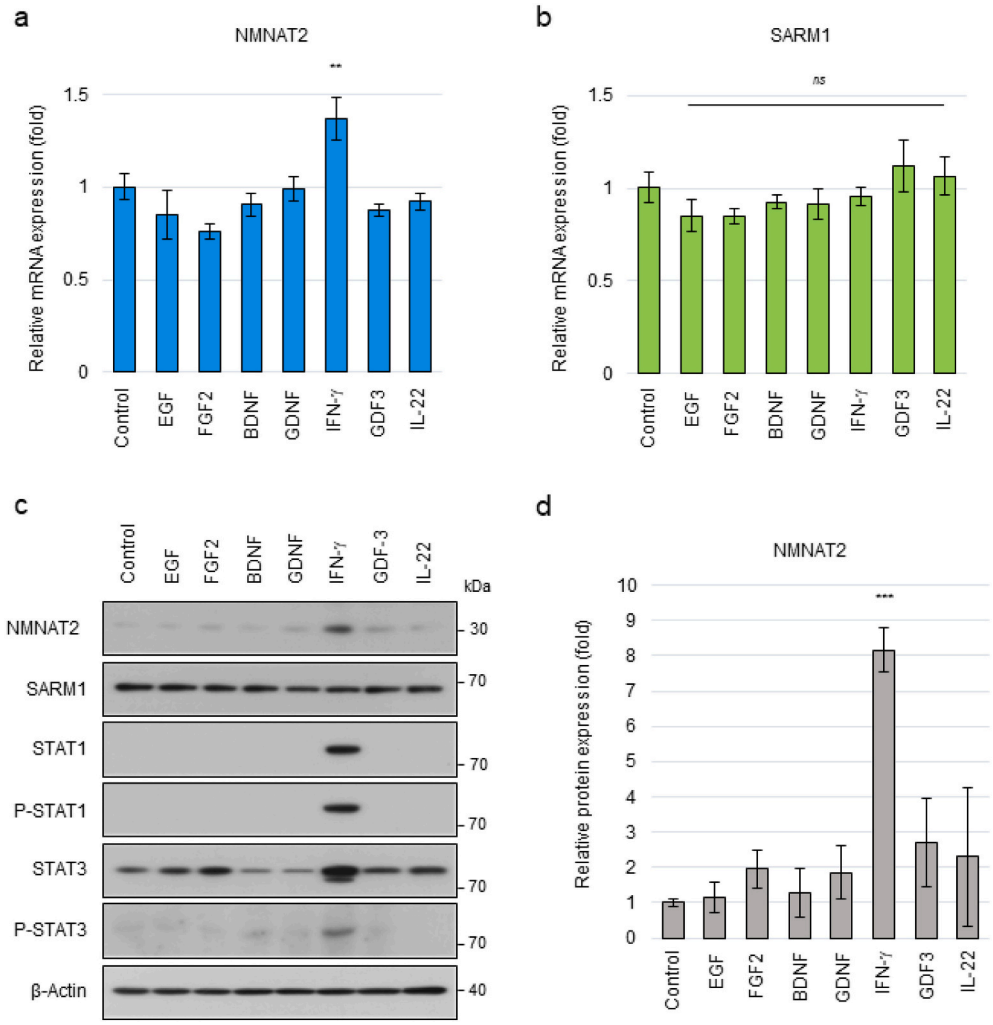

Fig. 1. Exploration of soluble factors that alter the expression of NAD^+-biosynthetic and NAD^+-consuming enzymes. Human NSCs were differentiated into neurons for 6 days. Then, the neurons were treated with the indicated soluble factors for 24 h. a, b. Relative mRNA expressions of *NMNAT2* and *SARM1*. Total RNAs prepared from the treated cells were used to analyze the gene expression by real-time qPCR. *GAPDH* RNA was used as a control for the analysis. c. Upregulation of NMNAT2 protein expression by IFN-γ. The neurons treated with the indicated cytokines were subjected to Western blot analysis using the indicated antibody. d. Quantitative analysis of NMNAT2 protein expression. **Significantly different from the control cells at $p < 0.01$; ***Significantly different from the control cells at $p < 0.001$; *ns*, not significant.

(Fig. 1(b and c)). Considering that IFN-γ regulates the JAK-STAT pathway after binding with the IFN receptor [32], we speculate that NMNAT2 would be induced by the pathway upon IFN-γ stimulation. We confirmed that IFN-γ treatment significantly increased the levels of the total and phosphorylated forms of STAT1 and STAT3 in iPSC-derived neurons (Fig. 1(c)). Based on these findings, we decided to further analyze the IFN-γ-mediated STAT signal in the regulation of NMNAT2 expression.

3.2. *IFN-γ increases the expression of NMNAT2 in a dose- and time-dependent manner*

There are several types of IFN, which control the expression of different genes via different receptors [33]. To specify IFN(s) that upregulate NMNAT2 expression in neurons, major types of IFN, IFN-α, IFN-β, and IFN-γ were studied. Among the IFNs used, IFN-γ induced the highest expression of NMNAT2 in iPSC-derived neurons, while IFN-β caused a slight increase in the expression of NMNAT2 and IFN-a had no effect on NMNAT2 expression (Fig. 2(a and c)). This pattern of increase in the expression of NMNAT2 was correlated with the activation states of both STAT1 and STAT3, in which only IFN-γ treatment increased the level of the total and phosphorylation form of STAT1 and STAT3. Although the increases in total STAT1 were similar at among the three IFNs, differences in phosphorylation were observed-i.e., a phosphorylation state was not observed with IFN-a, but phosphorylation was slightly elevated with IFN-β, and highly increased with IFN-γ (Fig. 2(c)). On the other hand, when different IFN treatments were used, none of these treatments had any effect on the SARM1 expression (Fig. 2(b and c)). To consolidate these findings, the WB result observed in the iPS-derived neuronal cells was also confirmed in another neuronal cell line, SH-SY5Y. As shown in Supplementary Fig. 1(a), NMNAT2 was induced by treatment with either IFN-β or IFN-γ in SH-SY5Y cells following a similar induction pattern as in the iPS-derived neuronal cells. Next, we investigated the effect of the treatment dose and duration of IFN-γ on the induction of NMNAT2 expression. IFN-γ induced an increase in NMNAT2 expression in a dose- (Fig. 2(d and f), Supplementary Fig. 1(b)) and time-dependent manner after treatment with IFN-γ (Fig. 2(g)). We then confirmed that the changes in the dose and treatment duration of IFN-γ did not affect the *SARM1* mRNA level (Fig. 2(e and h)). The effect of treatment duration was also examined by protein analysis. The expression level of NMNAT2 was increased around 24 h and the level was even sustained for another 24 h when the cells were treated with 100 ng/ml of IFN-γ. (Fig. 2(i)). In agreement with the increased pattern of NMNAT2, the expression of the STAT1 and STAT3 proteins were both highly elevated after 24 h treatment, and then both expressions experienced an additional slight increase over the subsequent 24 h. At this time, we confirmed that the other enzymes involved in NAD^+ synthesis and consumption (NMNAT1, NAMPT, and SARM1) resulted in almost no change in expression through the treatment duration with IFN-γ in the iPSC-derived neurons (Fig. 2(i)). An increase in NAMPT expression was observed in SH-SY5Y cells by IFN-γ treatment (Supplementary Fig. 1(a and b)). In light of the important role of STAT signaling

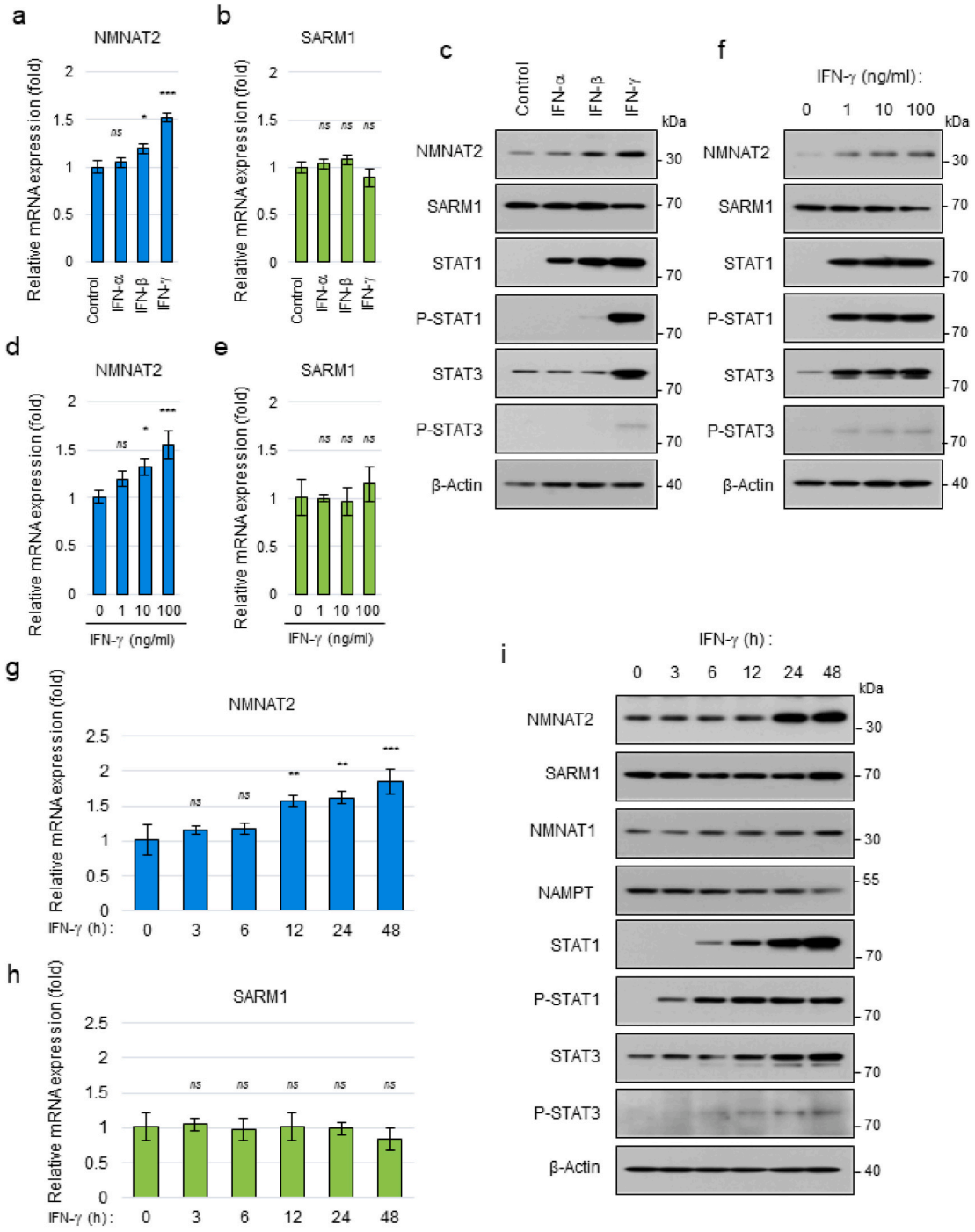

Fig. 2. IFN-γ induced NMNAT2 expression. a, b. Real-time qPCR analysis of *NMNAT2* and *SARM1* mRNA expression. Human iPSC-derived neurons were treated with 100 ng/ml of IFN-α, β or γ for 24 h. Total RNAs prepared from the treated cells were used to analyze the gene expression by real-time qPCR. c. IFN-γ induces NMNAT2 protein expression with activation of STAT signaling. The cell lysate of neurons treated with 100 ng/ml IFNs for 24 h were subjected to Western blot analysis using the indicated antibody. d-f. Dose dependence of NMNAT2 expression induced by IFN-γ. Human iPSC-derived neurons were treated with 0–100 ng/ml IFN-γ for 24 h. Total RNAs prepared from the cells were used to analyze for the mRNA expression of *NMNAT2* (d) and *SARM1* (e) by real-time qPCR. Cell lysates prepared from the neurons were subjected to Western blot analysis using the indicated antibody (f). g-i. Time course of NMNAT2 expression induced by IFN-γ treatment. Human iPSC-derived neurons were treated with 100 ng/ml IFN-γ from 0 to 48 h. The mRNA expressions of *NMNAT2* (g) and *SARM1* (h) were analyzed by real-time qPCR. The indicated protein expression was analyzed by Western blotting (i). *ns*, not significant; $*p < 0.05$; $**p < 0.01$; $***p < 0.001$.

on NMNAT2 induction in the neuronal cells, we expect that several soluble factors that activate the STAT pathway are also involved in NMNAT2 induction. Like INFs, interleukin-6 (IL-6) activates STAT signaling, and we therefore speculated that IL-6 also upregulates NMNAT2 expression. However, IL-6 treatment did not contribute to NMNAT2 expression in the iPSC-derived neurons (Supplementary Fig. 1 (c)). Because there was no obvious enhancement of the phosphorylation of STATs in response to IL-6, we considered that the level of expression of IL-6 receptors in the iPSC-derived neurons was extremely low. Collectively, these results suggest that NMNAT2 expression is positively regulated by activation of the STAT pathway, which is triggered by IFN-γ in neuronal cells.

3.3. IFN-γ upregulates NMNAT2 expression through STAT1/3 signaling

As shown in Fig. 2(c), IFN-γ, which elicited the greatest increase in NMNAT2 expression, induced higher-level activation of not only STAT1 but also STAT3 compared to other IFNs. Therefore, we examined the changes in IFN-γ-induced NMNAT2 expression in the cultured cells in the presence of the STAT3 inhibitors niclosamide and stattic. Treatment with niclosamide caused a dose-dependent decrease in NMNAT2 at both the mRNA and protein levels in the absence of IFN-γ, and both decreases also occurred in the presence of IFN-γ; that is, the NMNAT2 expression was effectively impeded by copresence with niclosamide (Fig. 3(a and b)). The expression levels of three other NAD^+-metabolizing enzymes, NMNAT1, NAMPT, and SARM1, were not affected by the inhibitor even at the high dose of 10 μM. For the IFN-γ-mediated STAT activation, we found that niclosamide at the highest concentration of 10 μM suppressed not only IFN-γ-induced STAT3 activation but also STAT1 activation (Fig. 3(b)). In SH-SY5Y cells, 1 μM niclosamide was sufficient to suppress STAT activation and NMNAT2 upregulation (Supplementary Fig. 1(d)). Under this inhibitory condition, it followed that similar patterns in expression dynamics for the proteins of our interest as seen in the iPS-derived neuronal cells (Fig. 3(b)) were observed, except in the case of NAMPT, the expression of which was decreased by the treatment with niclosamide in SH-SY5Y cells (Supplementary Fig. 1(d)). The use of another potent inhibitor, stattic, also gave similar results to those displayed in Fig. 3(a and b), where a dose-dependent decrease in NMNAT2 at the mRNA and protein levels was detected (Fig. 3(c and d)). These results indicate that STAT1/3 signaling upregulates NMNAT2 expression in neuronal cells.

3.4. STAT1/3 signaling increases NAD^+ levels in neurons

Next, we investigated whether STAT1/3 signaling would increase NAD^+ levels. IFN-γ had dose-dependently increased NAD^+ levels in iPSC-derived neurons (Fig. 4(a)) and in SH-SY5Y cells (Supplementary Fig. 2(a)). We then investigated whether NAD^+ levels were changed by treatment with the STAT3 inhibitor niclosamide. Treatment with niclosamide caused a decrease in NAD^+ levels in the absence of IFN-γ, and the decline also occurred in the presence of IFN-γ (Fig. 4(b)). We next used NMNAT2-overexpressing neurons to investigate whether only up-regulation of NMNAT2 is sufficient to increase NAD^+ levels (Fig. 4

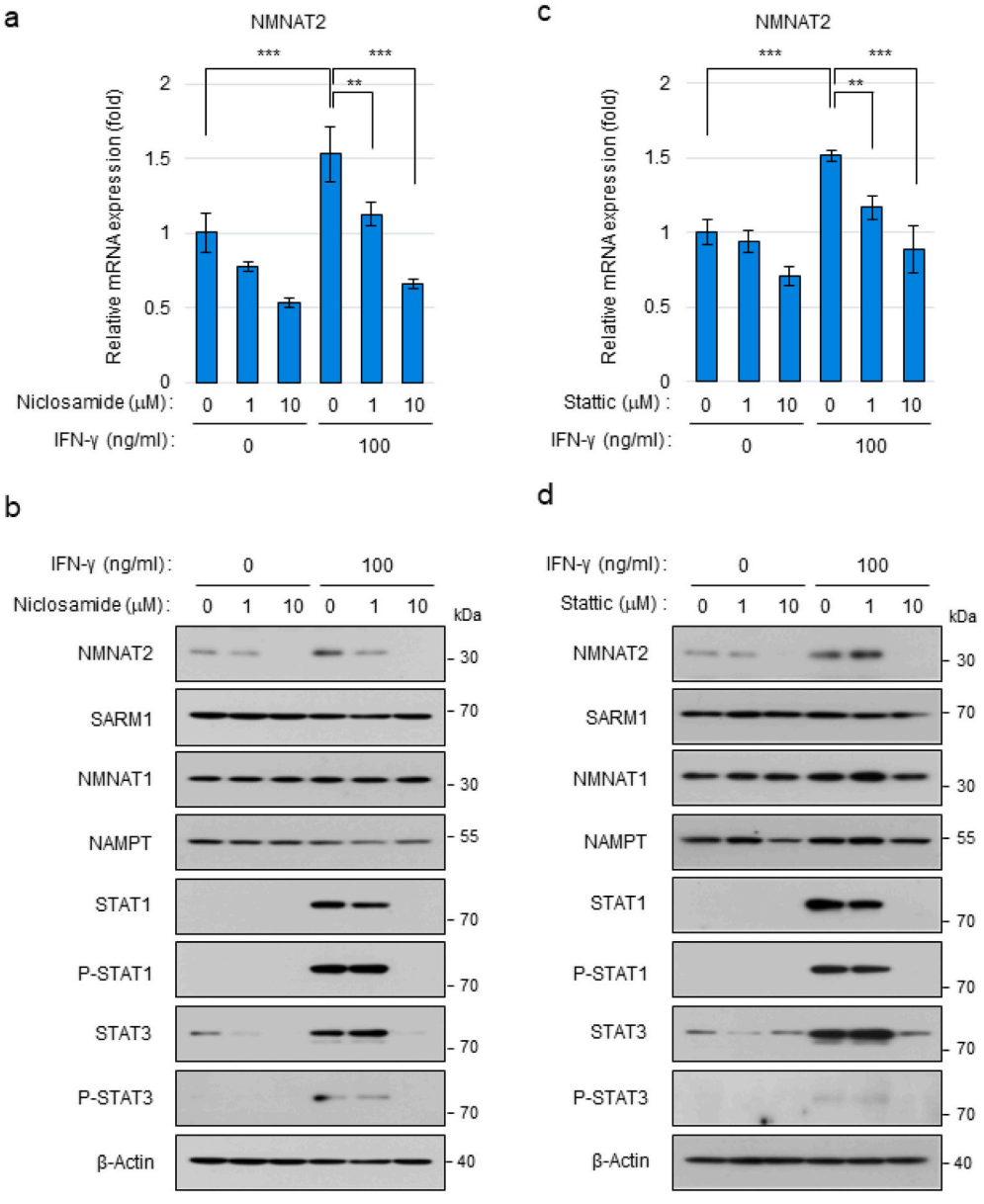

Fig. 3. Induction of NMNAT2 expression via STAT1/3 signaling. a, b. Niclosamide, a STAT3 inhibitor, suppressed NMNAT2 expression. Human iPSC-derived neurons were treated with 0–100 ng/ml IFN-γ and 0–10 μM niclosamide for 24 h. The mRNA expression of *NMNAT2* was analyzed by real-time qPCR (a). The indicated protein expression was analyzed by Western blotting. (b). c, d. Stattic, a STAT3 inhibitor, suppressed NMNAT2 expression. Human iPSC-derived neurons were treated with 0–100 ng/ml IFN-γ and 0–10 μM stattic for 24 h. The mRNA expression of *NMNAT2* was analyzed by real-time qPCR (c). The indicated protein expression was analyzed by Western blotting (d). $^{**}p < 0.01$; $^{***}p < 0.001$.

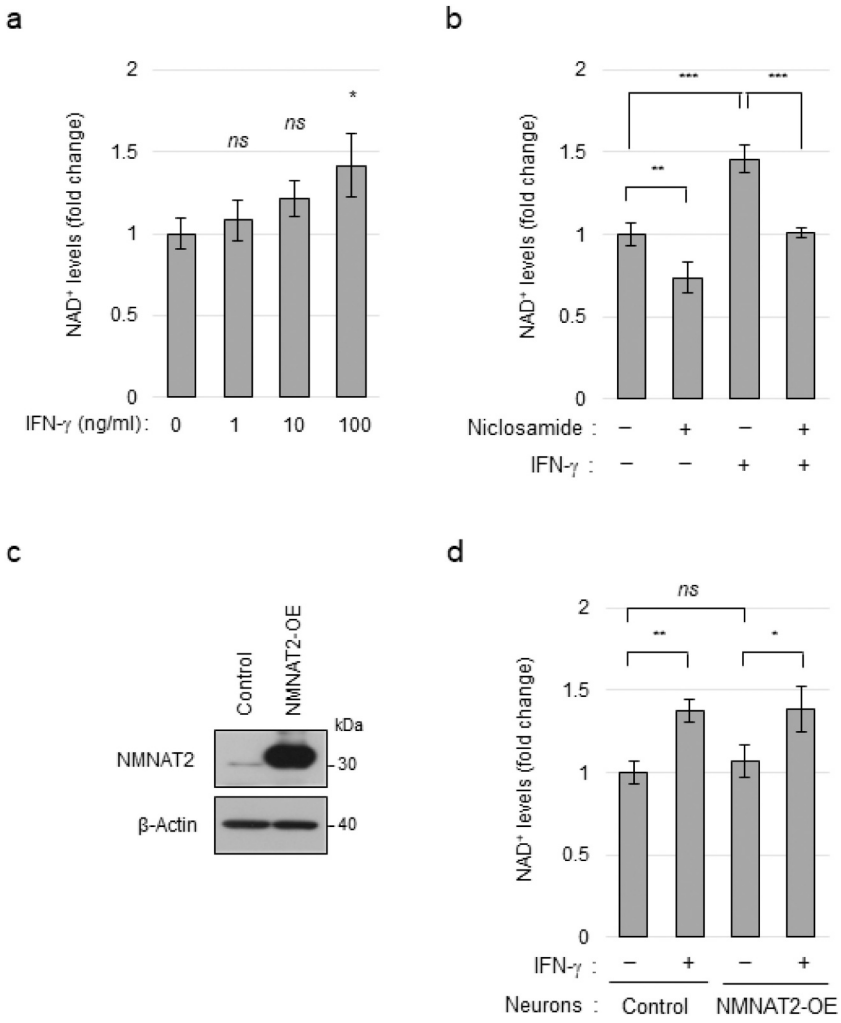

Fig. 4. STAT1/3 signaling upregulated NAD^+ production. a. Dose-dependent upregulation of NAD^+ production by IFN-γ. Human iPSC-derived neurons were treated with 0–100 ng/ml IFN-γ for 24 h, and then the intracellular NAD^+ levels were analyzed. b. Niclosamide, a STAT3 inhibitor, suppressed the NAD^+ production with or without IFN-γ. Human iPSC-derived neurons were treated with 0 or 100 ng/ml IFN-γ and 0 or 10 μM niclosamide for 24 h, and then the intracellular NAD^+ levels were analyzed. c. Confirmation of NMNAT2 overexpression in neurons. The indicated protein expression was analyzed by Western blotting. D. Confirmation of NAD^+ levels in NMNAT2-overexpressing neurons. Control neurons and NMNAT2-overexpressing neurons were treated with 0 or 100 ng/ml IFN-γ for 24 h, and then the intracellular NAD^+ levels were analyzed. *ns*, not significant; $*p < 0.05$; $**p < 0.01$; $***p < 0.001$.

(c)). Although the increase of NAD^+ levels was not observed in NMNAT2-overexpressing neurons in the absence of IFN-γ, the increase occurred in the presence of IFN-γ, as same as in control neurons (Fig. 4 (d)). These results suggest that the elevation of NAD^+ is not dependent on NMNAT2 expression, and STAT1/3 signaling is involved in the upregulation of NAD^+ synthesis in neurons.

3.5. *STAT1/3 signaling modestly suppresses vincristine-induced neurite degradation and cell death through induction of NMNAT2 expression and inactivation of SARM1*

The anticancer drug vincristine is for the clinical treatment of a variety of cancers. Vincristine exerts its antitumor effects by inhibiting microtubule polymerization, and thereby disrupting the microtubule-mediated spindle formation required for cancer cell division. On the other hand, vincristine also acts on the microtubules of nerve cells to induce axonal degeneration and cell death, causing CIPN. Vincristine is known to reduce the amount of NAD^+ in axons and induce CIPN by causing axonal degeneration [34]. To address these unwanted effects of an otherwise effective anticancer agent, we considered that IFN-γ-mediated STAT1/3 activation might be useful to ameliorate CIPN. To investigate this possibility, we first added vincristine to a culture of human iPSC-derived neurons and investigated the proteins of our interest for their expression and activation dynamics. As shown in Fig. 5(a), a marked reduction of NMNAT2 was observed 12 h after the treatment with vincristine, and thereafter the band disappeared. NMNAT1, a family member of NMNAT, decreased 24 h after the stimulus. On the other hand, no obvious change in the protein level of SARM1 was observed by vincristine exposure, but SARM1 phosphorylation was detected and peaked at 24 h after vincristine addition. This finding was well consistent with our previous observation that SARM1 was phosphorylated by JNK in response to several stress conditions, and the phosphorylation in turn enhanced the enzymatic activity of SARM1 to cleave NAD^+ [24]. In fact, activation of JNK was confirmed based on the observation of phosphorylation of JNK and c-Jun, a representative JNK substrate, in this experimental setting (Fig. 5 (a)). In parallel with the time-dependent decrease in NMNAT2 and increase of phosphorylation of JNK, c-Jun and SARM1, the bands of neurofilaments (NF-L and NF-M), which are axonal main components, showed a time-dependent reduction. At 24 h and 48 h after the stimulation, the bands were absent and cleaved caspase 3, a central marker of apoptosis, was detected. These results indicate that axonal degeneration and subsequent apoptotic cell death are induced in neuronal cells by treatment with vincristine.

Next, we investigated whether IFN-γ-mediated STAT1/3 activation could suppress vincristine-induced cell death and axonal degeneration. The cell-based assay revealed that IFN-γ has an ability to partially suppress the vincristine-induced neuronal cell death in a dose-dependent manner (Fig. 5(b)). A similar inhibitory effect was also observed in SH-SY5Y cells (Supplementary Fig. 2(b)). The machinery by which IFN-γ inhibits vincristine-induced cell death and axonal degeneration was then investigated by WB analysis (Fig. 5(c)). Notably, IFN-γ treatment restored NMNAT2 to the physiological level from the severely reduced level caused by vincristine treatment. In addition, the significant vincristine-mediated phosphorylation of SARM1 was also reduced by the presence of IFN-γ in culture. This was probably due to the ability of

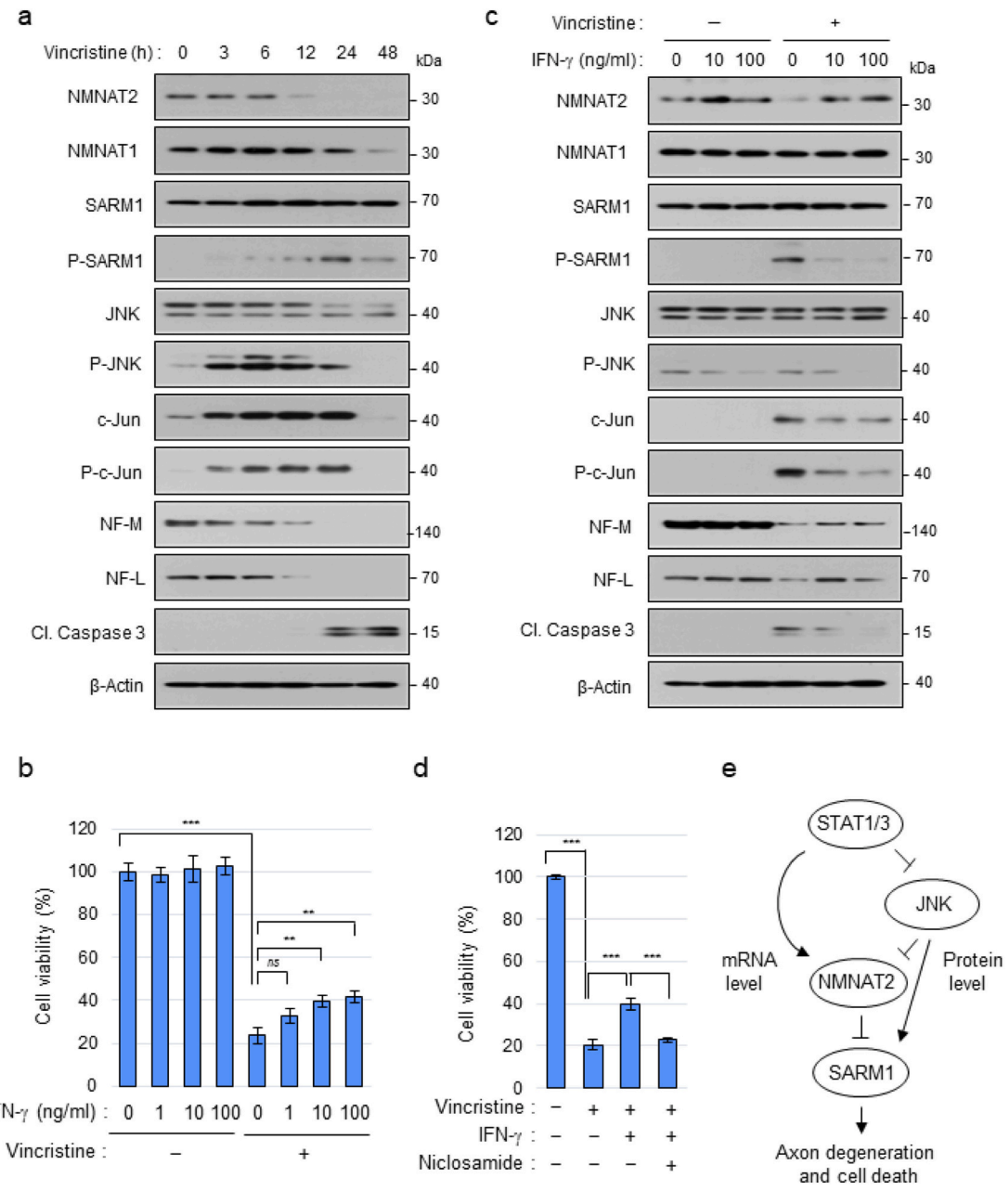

Fig. 5. STAT1/3 signaling modestly suppressed vincristine-induced cell death by upregulation of NMNAT2 expression and inactivation of SARM1. a. Time course of protein expression after treatment with vincristine. Human iPSC-derived neurons were treated with 50 nM vincristine from 0 to 48 h. The cell lysates were subjected to Western blot analysis using the indicated antibody. b. IFN-γ dose-dependently suppressed vincristine-induced cell death. Human iPSC-derived neurons were treated with 0–100 ng/ml IFN-γ for 24 h and further treated with 0 or 50 nM vincristine for another 24 h in the presence of IFN-γ, and then the cell viability was analyzed. c. IFN-γ-mediated STAT1/3 activation partially suppressed vincristine-induced neurite degradation and cell death. Human iPSC-derived neurons were treated with 0–100 ng/ml IFN-γ for 24 h and further treated with 0 or 50 nM vincristine for another 24 h in the presence of IFN-γ. The cell lysates were subjected to Western blot analysis using the indicated antibody. d. Niclosamide, a STAT3 inhibitor, canceled the cell death-inhibiting effects of IFN-γ. Human iPSC-derived neurons were treated with IFN-γ (0 or 100 ng/ml) for 24 h and further treated with vincristine (0 or 50 nM) and niclosamide (0 or 10 mM) for another 24 h in the presence of IFN-γ, and then the cell viability was analyzed. e. A working model for suppression of axon degeneration and cell death by STAT1/3 signaling. *ns*, not significant; $^{**}p < 0.01$; $^{***}p < 0.001$.

IFN-γ-STAT signaling to inhibit JNK activation since we confirmed that IFN-γ treatment decreased the phosphorylation of JNK and c-Jun (Fig. 5 (c)), while niclosamide treatment increased the phosphorylation of c-Jun (Supplementary Fig. 1(e)). It has also been reported that IFN-γ suppresses JNK activity via endogenous nitric oxide production [35]. Consistent with these results and report, we observed that the vincristine-induced reduction of neurofilaments (NF-L and NF-M) and vincristine-induced increases in cleaved caspase 3 were modestly suppressed by the treatment with IFN-γ (Fig. 5(c) and Supplementary Fig. 3 (a and b)). To observe the protective effects of STAT1/3 signaling against the vincristine-mediated axon degeneration more directly, we cultured iPSC-derived neurons in compartmentalized microfluidic chambers that allow independent manipulation of cell bodies and axons (Supplementary Fig. 3(c)). Geisler et al. used these chambers to show that vincristine stimulates an axon-autonomous degenerative process [29]. Using this chamber, we observed that axon fragmentation occurred by treating the axonal side with vincristine, and IFN-γ-mediated STAT1/3 activation partially suppressed this event (Supplementary

Fig. 3(d and e)). The cell-protective effect of IFN-γ against the vincristine-mediated cell injury was canceled by using the STAT3 inhibitor niclosamide (Fig. 5(d) and Supplementary Fig. 2(c)). Next, we established neurons that downregulated NMNAT2 and overexpressed SARM1 to investigate whether NMNAT2 and SARM1 are involved in the vincristine-induced cell death (Supplementary Fig. 4(a)). The cell-protective effect of IFN-γ-mediated STAT1/3 activation was mostly canceled by the downregulation of NMNAT2 and the upregulation of SARM1 (Supplementary Fig. 4(b)). These results indicate that activation of the STAT1/3 signaling contributes to suppression of the vincristine-induced axonal degeneration and cell death through induction of NMNAT2 expression and inhibition of SARM1 phosphorylation in neuronal cells (Fig. 5(e)).

4. Discussion

In this study, we revealed an important new role of STAT1/3 signaling in neuronal protection. We showed that IFN-γ-mediated STAT1/3 activation upregulated the expression of the NAD^+ synthase NMNAT2 and inversely suppressed the activation of the NAD^+-consuming enzyme SARM1. These events are exerted by activation of the STAT1/3 pathway and inactivation of the JNK pathway. These findings should be helpful in any renewed attempts to develop a treatment for CIPN since STAT1/3 activation suppressed vincristine-induced axonal degradation and cell death, although not completely. In addition to CIPN, reduced NAD^+ levels play an important role in many other types of neurodegenerative diseases, and thus an NAD^+-regulatory strategy based on our findings might also prevent the progression of these other neurodegenerative conditions.

The coenzyme NAD^+ is an essential factor in life. The use of NAD^+ is pleiotropic; that is, NAD^+ is required for oxidation/reduction reactions, mediating glycolysis and oxidative phosphorylation in mitochondria, and energy metabolism [36]. In addition to these coenzymatic roles, NAD^+ also functions as a cofactor that is required for the activation of several proteins, such as PARP, a DNA repair protein, and the deacetylase Sirtuin, an anti-aging protein. It has been reported that the NAD^+-bound active Sirtuin suppresses not only the appearance of aging phenotypes of organisms but also the progression of various diseases, eventually leading to increased healthy longevity [37]. Thus, NAD^+ plays a crucial role in various physiological life phenomena as well as disease phenomena via coenzymatic and cofactor roles. As a result, when severe, sustainable reduction of NAD^+ occurs, life is threatened because of mal functions in life events that will progress to senescence-relevant diseases. NAD^+ levels are known to decrease in various tissues with aging [38]. Thus, our discovery of an STAT1/3-triggered NAD^+-maintenance machinery in cells, consisting of STAT-mediated upregulation of NMNAT2 expression and STAT-mediated suppression of SARM1 activation, should contribute to an improved understanding of the senescence-relevant harmful changes in the aging body at the cellular and molecular levels.

In this study, we found that IFN-γ-mediated STAT1/3 activation increased NMNAT2 expression at both transcriptional (Fig. 1(a)) and protein levels (Fig. 1(c and d)). Walker et al. reported that MAPK signaling promotes NMNAT2 turnover and that the knockdown of MKK4/7 upstream of JNK increased NMNAT2 at the protein level [39]. Since IFN-γ treatment decreased the phosphorylation of JNK, c-Jun, and SARM1 (Fig. 5(c)), it is conceivable that IFN-γ-STAT1/3 signaling suppresses the JNK pathway in human iPSC-derived neurons. We also found that the treatment with the STAT3 inhibitor niclosamide increased the phosphorylation of c-Jun (Supplementary Fig. 1(e)). Thus, JNK suppression is one of the mechanisms of NMNAT2 induction at protein levels in the IFN-γ treatment setting in neuronal cells. Taken together, our results suggest the pathway schematic shown in Fig. 5(e), in which STAT1/3-JNK signaling contributes to the regulation of NMNAT2 expression at both transcriptional and protein levels.

Next, we will consider the difference in the intracellular reaction in response to IFN-γ between human iPSC-derived neuronal cells and human neuroblastoma SH-SY5Y cells. NAMPT expression was somehow increased in SHSY-5Y cells but not in human iPSC-derived neuronal cells after the addition of IFN-γ (Supplementary Fig. 1(a and b)). One reason for this result may have been the different expression levels of STAT3 between these cell types since STAT3 is highly upregulated in a variety of cancer cells compared to normal cells. Like NMNAT2, STAT3 may be involved in NAMPT induction since the IFN-γ-mediated upregulation of NAMPT was suppressed by the STAT3 inhibitor niclosamide in SH-SY5Y cells (Supplementary Fig. 1(d)). It may be that the increased expression of STAT3 in SH-SY5Y cells compared to STAT3 expression in iPSC-derived normal neuronal cells acts to increase both NAMPT and NMNAT2 in response to IFN-γ, which may mirror the higher level of increase in NAD^+ and greater ability to resist vincristine-induced cell death in SH-SY5Y cells than normal cells after stimulation with IFN-γ (Supplementary Fig. 2). Although IFN-γ treatment increased NMNAT2 expression as well as NAD^+ levels in iPSC-derived neurons (Fig. 4(a)), the single overexpression procedure of NMNAT2 was not associated with the sufficient increase in NAD^+ levels (Fig. 4(d)). In this setting, however, treatment with niclosamide decreased the NAD^+ levels (Fig. 4(b)). Since NMNATs are not the rate limiting enzymes in the NAD^+ salvage pathway, the IFN-γ-STAT1/3 axis may affect NAMPT activation to increase NAD^+ levels, otherwise via still unidentified path(s), in iPSC-derived neurons.

Although we have shown that IFN-γ-STAT1/3 signaling suppresses vincristine-induced axonal degeneration and cell death in neuronal cells *in vitro*, it remains uncertain whether these results directly mirror the situation *in vivo*, since the neural milieu is much more complex than a simple *in vitro* culture system. For example, the *in vivo* environment would contain many cell types other than neuronal cells, and these cells would inevitably be affected by IFN-γ and undergo mutual cross-talk. In addition, IFN-γ can induce inflammation *in vivo*, primarily when targeted to immune cells, and such inflammation may compromise neuronal cells. Therefore, neuronal cells may have evolved the IFN-γ-STAT1/3-mediated cell survival system revealed herein in order to protect against inflammatory threats in the living body. The findings of several previous reports support this idea. For instance, Victorio et al. reported that the rate of neurodegeneration caused by sciatic nerve transection is highly increased by IFN-γ deficiency [40]. Bareyre et al. showed that STAT3 is involved in axonal regeneration after axotomy [41]. In addition, Selvaraj et al. reported that STAT3 activation rescued axonal degeneration in a progressive motor neuropathy model [42]. Thus, it is clear that the IFN-γ-STAT1/3 pathway functions to protect axons and neuronal cells even in the complex *in vivo* milieu. It is conceivable that methods to manipulate STAT1/3 activity to suppress NAD^+ reduction may become a valuable strategy to prevent or alleviate CIPN and possibly other neurodegenerative diseases.

5. Conclusion

STAT1/3 signaling induces NMNAT2 expression while simultaneously suppressing SARM1 phosphorylation via JNK inactivation, and both these actions contribute to suppression of axonal degeneration and cell death.

Funding

This work was supported by a JSPS KAKENHI Grant for Scientific Research C (no. 22K06884 to H. M.) and a Japan Agency for Medical Research and Development Grant (no. 22ym0126810j0001 to H. M.).

CRediT authorship contribution statement

Hitoshi Murata: Conceptualization, Methodology, Validation, Formal analysis, Investigation, Writing – original draft, Writing – review & editing, Funding acquisition. **Yu Yasui:** Validation, Formal analysis,

Investigation, Visualization. **Kazuma Oiso:** Investigation, Validation. **Toshiki Ochi:** Methodology, Investigation. **Nahoko Tomonobu:** Resources. **Ken-ichi Yamamoto:** Investigation. **Rie Kinoshita:** Resources, Supervision. **Masakiyo Sakaguchi:** Writing – review & editing, Supervision, Project administration.

Declaration of Competing Interest

The authors declare that they have no conflicts of interest with respect to the contents of this article.

Data availability

Data will be made available on request.

Acknowledgments

The NAD^+ assay using FlexStation 3 was supported by the Central Research Laboratory of the Okayama University Medical School.

Appendix A. Supplementary data

Supplementary data to this article can be found online at https://doi.org/10.1016/j.cellsig.2023.110717.

References

[1] M.P. Coleman, A. Hoke, Programmed axon degeneration: from mouse to mechanism to medicine, Nat. Rev. Neurosci. 21 (4) (2020) 183–196.
[2] J. Gilley, M.P. Coleman, Endogenous Nmnat2 is an essential survival factor for maintenance of healthy axons, PLoS Biol. 8 (1) (2010), e1000300.
[3] M.D. Figley, A. DiAntonio, The SARM1 axon degeneration pathway: control of the NAD(+) metabolome regulates axon survival in health and disease, Curr. Opin. Neurobiol. 63 (2020) 59–66.
[4] N.Z. Gcwensa, D.L. Russell, R.M. Cowell, L.A. Volpicelli-Daley, Molecular mechanisms underlying synaptic and axon degeneration in Parkinson's disease, Front. Cell. Neurosci. 15 (2021), 626128.
[5] N. Salvadores, M. Sanhueza, P. Manque, F.A. Court, Axonal degeneration during aging and its functional role in neurodegenerative disorders, Front. Neurosci. 11 (2017) 451.
[6] Y.O. Ali, D. Li-Kroeger, H.J. Bellen, R.G. Zhai, H.C. Lu, NMNATs, evolutionarily conserved neuronal maintenance factors, Trends Neurosci. 36 (11) (2013) 632–640.
[7] M. Schweiger, K. Hennig, F. Lerner, M. Niere, M. Hirsch-Kauffmann, T. Specht, C. Weise, S.L. Oei, M. Ziegler, Characterization of recombinant human nicotinamide mononucleotide adenylyl transferase (NMNAT), a nuclear enzyme essential for NAD synthesis, FEBS Lett. 492 (1–2) (2001) 95–100.
[8] S. Milde, J. Gilley, M.P. Coleman, Subcellular localization determines the stability and axon protective capacity of axon survival factor Nmnat2, PLoS Biol. 11 (4) (2013), e1001539.
[9] Y. Sasaki, T. Araki, J. Milbrandt, Stimulation of nicotinamide adenine dinucleotide biosynthetic pathways delays axonal degeneration after axotomy, J. Neurosci. 26 (33) (2006) 8484–8491.
[10] A. Loreto, C.S. Hill, V.L. Hewitt, G. Orsomando, C. Angeletti, J. Gilley, C. Lucci, A. Sanchez-Martinez, A.J. Whitworth, L. Conforti, F. Dajas-Bailador, M.P. Coleman, Mitochondrial impairment activates the Wallerian pathway through depletion of NMNAT2 leading to SARM1-dependent axon degeneration, Neurobiol. Dis. 134 (2020), 104678.
[11] S. Milde, A.N. Fox, M.R. Freeman, M.P. Coleman, Deletions within its subcellular targeting domain enhance the axon protective capacity of Nmnat2 in vivo, Sci. Rep. 3 (2013) 2567.
[12] S. Milde, M.P. Coleman, Identification of palmitoyltransferase and thioesterase enzymes that control the subcellular localization of axon survival factor nicotinamide mononucleotide adenylyltransferase 2 (NMNAT2), J. Biol. Chem. 289 (47) (2014) 32858–32870.
[13] D.W. Summers, J. Milbrandt, A. DiAntonio, Palmitoylation enables MAPK-dependent proteostasis of axon survival factors, Proc. Natl. Acad. Sci. U. S. A. 115 (37) (2018) E8746–E8754.
[14] Y. Yamagishi, M. Tessier-Lavigne, An atypical SCF-like ubiquitin ligase complex promotes Wallerian degeneration through regulation of axonal Nmnat2, Cell Rep. 17 (3) (2016) 774–782.
[15] M. Desbois, O. Crawley, P.R. Evans, S.T. Baker, I. Masuho, R. Yasuda, B. Grill, PAM forms an atypical SCF ubiquitin ligase complex that ubiquitinates and degrades NMNAT2, J. Biol. Chem. 293 (36) (2018) 13897–13909.
[16] A.J. Covarrubias, R. Perrone, A. Grozio, E. Verdin, NAD(+) metabolism and its roles in cellular processes during ageing, Nat. Rev. Mol. Cell Biol. 22 (2) (2021) 119–141.
[17] K. Mao, G. Zhang, The role of PARP1 in neurodegenerative diseases and aging, FEBS J. 289 (8) (2022) 2013–2024.
[18] A. De Flora, E. Zocchi, L. Guida, L. Franco, S. Bruzzone, Autocrine and paracrine calcium signaling by the CD38/NAD+/cyclic ADP-ribose system, Ann. N. Y. Acad. Sci. 1028 (2004) 176–191.
[19] J.M. Osterloh, J. Yang, T.M. Rooney, A.N. Fox, R. Adalbert, E.H. Powell, A. E. Sheehan, M.A. Avery, R. Hackett, M.A. Logan, J.M. MacDonald, J.S. Ziegenfuss, S. Milde, Y.J. Hou, C. Nathan, A. Ding, R.H. Brown Jr., L. Conforti, M. Coleman, M. Tessier-Lavigne, S. Zuchner, M.R. Freeman, dSarm/Sarm1 is required for activation of an injury-induced axon death pathway, Science 337 (6093) (2012) 481–484.
[20] K. Essuman, D.W. Summers, Y. Sasaki, X. Mao, A. DiAntonio, J. Milbrandt, The SARM1 toll/Interleukin-1 receptor domain possesses intrinsic NAD(+) cleavage activity that promotes pathological axonal degeneration, Neuron 93 (6) (2017) 1334–1343 e5.
[21] M. Bratkowski, T. Xie, D.A. Thayer, S. Lad, P. Mathur, Y.S. Yang, G. Danko, T. C. Burdett, J. Danao, A. Cantor, J.A. Kozak, S.P. Brown, X. Bai, S. Sambashivan, Structural and mechanistic regulation of the pro-degenerative NAD hydrolase SARM1, Cell Rep. 32 (5) (2020), 107999.
[22] M.D. Figley, W. Gu, J.D. Nanson, Y. Shi, Y. Sasaki, K. Cunnea, A.K. Malde, X. Jia, Z. Luo, F.K. Saikot, T. Mosaiab, V. Masic, S. Holt, L. Hartley-Tassell, H. Y. McGuinness, M.K. Manik, T. Bosanac, M.J. Landsberg, P.S. Kerry, M. Mobli, R. O. Hughes, J. Milbrandt, B. Kobe, A. DiAntonio, T. Ve, SARM1 is a metabolic sensor activated by an increased NMN/NAD(+) ratio to trigger axon degeneration, Neuron 109 (7) (2021) 1118–1136 e11.
[23] Y. Shi, P.S. Kerry, J.D. Nanson, T. Bosanac, Y. Sasaki, R. Krauss, F.K. Saikot, S. E. Adams, T. Mosaiab, V. Masic, X. Mao, F. Rose, E. Vasquez, M. Furrer, K. Cunnea, A. Brearley, W. Gu, Z. Luo, L. Brillault, M.J. Landsberg, A. DiAntonio, B. Kobe, J. Milbrandt, R.O. Hughes, T. Ve, Structural basis of SARM1 activation, substrate recognition, and inhibition by small molecules, Mol. Cell 82 (9) (2022) 1643–1659 e10.
[24] H. Murata, C.C. Khine, A. Nishikawa, K.I. Yamamoto, R. Kinoshita, M. Sakaguchi, C-Jun N-terminal kinase (JNK)-mediated phosphorylation of SARM1 regulates NAD(+) cleavage activity to inhibit mitochondrial respiration, J. Biol. Chem. 293 (49) (2018) 18933–18943.
[25] L.A. Colvin, Chemotherapy-induced peripheral neuropathy: where are we now? Pain 160 (Suppl. 1) (2019) S1–S10.
[26] R.A. Slivicki, Y.O. Ali, H.C. Lu, A.G. Hohmann, Impact of genetic reduction of NMNAT2 on chemotherapy-induced losses in cell viability in vitro and peripheral neuropathy in vivo, PLoS One 11 (1) (2016), e0147620.
[27] S. Geisler, R.A. Doan, A. Strickland, X. Huang, J. Milbrandt, A. DiAntonio, Prevention of vincristine-induced peripheral neuropathy by genetic deletion of SARM1 in mice, Brain 139 (Pt 12) (2016) 3092–3108.
[28] E. Turkiew, D. Falconer, N. Reed, A. Hoke, Deletion of Sarm1 gene is neuroprotective in two models of peripheral neuropathy, J. Peripher. Nerv. Syst. 22 (3) (2017) 162–171.
[29] S. Geisler, R.A. Doan, G.C. Cheng, A. Cetinkaya-Fisgin, S.X. Huang, A. Hoke, J. Milbrandt, A. DiAntonio, Vincristine and bortezomib use distinct upstream mechanisms to activate a common SARM1-dependent axon degeneration program, JCI Insight 4 (17) (2019).
[30] M. Sakaguchi, M. Watanabe, R. Kinoshita, H. Kaku, H. Ueki, J. Futami, H. Murata, Y. Inoue, S.A. Li, P. Huang, E.W. Putranto, I.M. Ruma, Y. Nasu, H. Kumon, N. H. Huh, Dramatic increase in expression of a transgene by insertion of promoters downstream of the cargo gene, Mol. Biotechnol. 56 (7) (2014) 621–630.
[31] Y. Kanda, Investigation of the freely available easy-to-use software 'EZR' for medical statistics, Bone Marrow Transplant. 48 (3) (2013) 452–458.
[32] X. Hu, J. Li, M. Fu, X. Zhao, W. Wang, The JAK/STAT signaling pathway: from bench to clinic, Sig. Transduct. Target Ther. 6 (1) (2021) 402.
[33] L.C. Platanias, Mechanisms of type-I- and type-II-interferon-mediated signalling, Nat. Rev. Immunol. 5 (5) (2005) 375–386.
[34] Y. Fukuda, Y. Li, R.A. Segal, A mechanistic understanding of axon degeneration in chemotherapy-induced peripheral neuropathy, Front. Neurosci. 11 (2017) 481.
[35] H.S. Park, S.H. Huh, M.S. Kim, S.H. Lee, E.J. Choi, Nitric oxide negatively regulates c-Jun N-terminal kinase/stress-activated protein kinase by means of S-nitrosylation, Proc. Natl. Acad. Sci. U. S. A. 97 (26) (2000) 14382–14387.
[36] N. Xie, L. Zhang, W. Gao, C. Huang, P.E. Huber, X. Zhou, C. Li, G. Shen, B. Zou, NAD(+) metabolism: pathophysiologic mechanisms and therapeutic potential, Sig. Transduct. Target Ther. 5 (1) (2020) 227.
[37] A. Satoh, S.I. Imai, L. Guarente, The brain, sirtuins, and ageing, Nat. Rev. Neurosci. 18 (6) (2017) 362–374.
[38] M.R. McReynolds, K. Chellappa, J.A. Baur, Age-related NAD(+) decline, Exp. Gerontol. 134 (2020), 110888.
[39] L.J. Walker, D.W. Summers, Y. Sasaki, E.J. Brace, J. Milbrandt, A. DiAntonio, MAPK signaling promotes axonal degeneration by speeding the turnover of the axonal maintenance factor NMNAT2, Elife 6 (2017).
[40] S.C. Victorio, L.A. Havton, A.L. Oliveira, Absence of IFNgamma expression induces neuronal degeneration in the spinal cord of adult mice, J. Neuroinflammation 7 (2010) 77.
[41] F.M. Bareyre, N. Garzorz, C. Lang, T. Misgeld, H. Buning, M. Kerschensteiner, In vivo imaging reveals a phase-specific role of STAT3 during central and peripheral nervous system axon regeneration, Proc. Natl. Acad. Sci. U. S. A. 108 (15) (2011) 6282–6287.
[42] B.T. Selvaraj, N. Frank, F.L. Bender, E. Asan, M. Sendtner, Local axonal function of STAT3 rescues axon degeneration in the pmn model of motoneuron disease, J. Cell Biol. 199 (3) (2012) 437–451.